Computational Hydraulic Analysis of APR1400Reactor Coolant Pump

Ja Y. Gu[a], Kune Y. Suh[a,b*]
[a]*PHILOSOPHIA, Inc., 599 Gwanak-Ro, Gwanak-Gu, Seoul, 151-744, Korea*
[b]*Seoul National Univ., 599 Gwanak-Ro, Gwanak-Gu, Seoul, 151-744, Korea*
**Corresponding author: kysuh@snu.ac.kr*

1. Introduction

A preceding study [1] of blades of the reactor coolant pump (RCP) for the Advanced Power Reactor 1400 (APR1400) helps the blade performance to be estimated. The tendency to actual experiment results also can be predicted with the analysis results. The exact values, however, are not predicted since other constituents other than the blades and passage are simplified for the sake of computational analysis.

In this study the hydraulic performance of the RCP model reflecting actual shape such as inlet, outlet and casing is analyzed by using computational analysis and compared with experiment results. The effects of rapid changes of pathway on the back of diffusers are prospected as well.

2. CFD analysis

2.1. Pump modeling and meshing

The model is divided into two parts since the analysis is performed with the similar model to the actual pump. One is a part including both impeller and diffuser blades and another one a casing part on the back of diffuser. This division is profitable for analysis because the blade part applies both fixed and rotating frame of reference, but the casing part uses just fixed reference frame. Therefore, some computations become simple for just one of two parts.

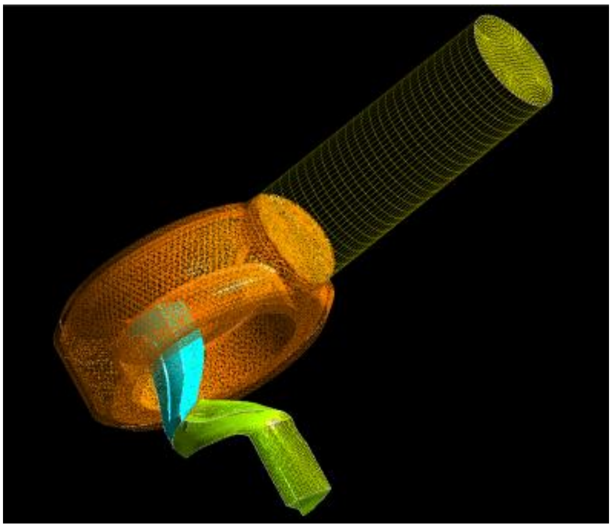

Fig. 1 Shape and the structure of grid systems of the RCP assembly.

Figure 1 shows the shape of the RCP assembly and illustrates how the grids of each part are made. The girds of two parts are generated with different meshing techniques. For the blade part a structured grid system is used at all area and only hexahedron grids are filled. For the casing part various grids are employed such as pyramid, prism, tetrahedron and hexahedron. Nodes, which are points on crossed grid lines, are shared on an interface where two different parts face to each other as the casing outlet is connected a pipe for discharge in Fig. 1. Theis sharing has some advantages regarding transmitting values calculated prior to an interface. Finally total number of grids for the analysis model is 788,670 elements.

2.2. Numerical Method [2,3]

The computational analysis is executed by ANSYS CFX® by employing the Reynolds averaged Navier-Stokes (RANS) equations as governing equations to examine incompressible turbulent flow. The high resolution scheme is used as derivation technique, while the Shear Stress Transport (SST) based on k-ω model is used to account for turbulence. Also the Total Energy is for the heat transfer. The boundary conditions are based on the nominal operating condition of APR1400 as listed in Table I. The inlet and outlet point is located at the position similar to actual measuring points.

Table I:. RCP Boundary Conditions

Parameter	Design	Operation
Inlet total pressure [MPa]	17.6	15.6
Temperature [°C]	343	290.6
Outlet mass flow rate [m^3/s]	5719.44	
Working fluid	Water	

3. Results and discussion

The charts shown in Fig. 2 and Fig. 3 illustrate the performance curves for the RCP. The performance curves from analysis results including the casing part predict more accurately the experiment values than the performance curves of just a blade part. The efficiency, η is calculated as following equation

$$\eta = \frac{\rho g Q H}{P_{shaft}} \qquad (1)$$

Note that ρ is density, g acceleration of gravity, Q flow, H head and P_{shaft} shaft power.

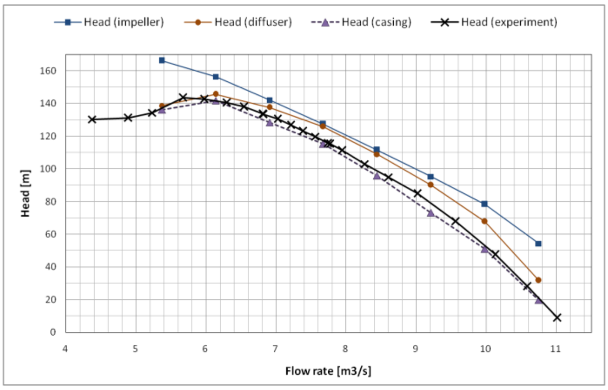

Fig. 1 Performance curves: head.

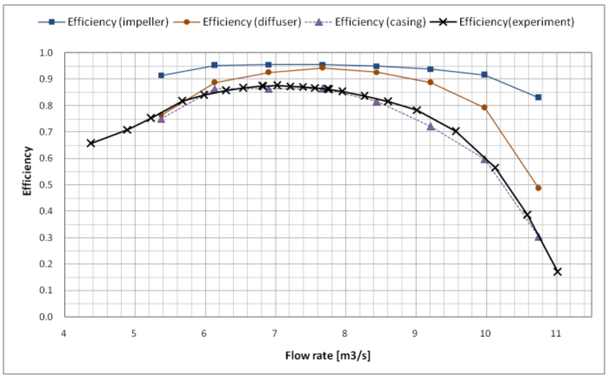

Fig. 2 Performance curves: efficiency.

At any region of flow rate the final results seem to trace accurately experimental data though loss rate at boundary of composition such as impeller, diffuser and casing is different respectively. The losses from impeller to diffuser are more than those during a casing at flow rate where is the off-design points. The loss around the flow rate after the design point, however, is mostly owing to it in the casing.

There are a many kinds of losses which are occurred on blades near flow rate of off-design points. A generally most causing big effect is separation, cavitations and secondary flow. In this case losses from separation and secondary flow are primary causes. Since the head and efficiency near the design point satisfy the design conditions the blades for impeller and diffuser is sufficiently designed [1].

The loss which gets from casing is mainly on account of a shape change and friction with casing wall. It is visible from Fig. 4 that the pressure drop takes place in the chamber of casing after out of diffuser and in the pipe of casing, especially near its wall. A plane around blades is on mid-span of impeller and diffuser. The other planes for the casing are located on a center section. Arrows on planes denote velocity vectors. Note that two legends are applied to each plane which shows pressure distributions.

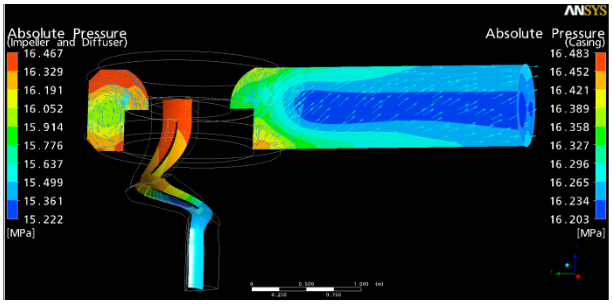

Fig. 4 Absolute pressure distribution on virtual planes in the RCP

4. Conclusions

This study has furthered the previous work from the analysis of performances of just blades of the RCP to one of total geometry for APR1400. The performance through the analysis technique in this study estimates perfectly actual result from experiment within an average error of one percent.

Consequently, the design for blades and casing can be estimated as it satisfies the hydraulic and structural goals. Additionally, the analysis technique is reliable to validate the RCP's hydraulic performance for the APR1400.

The result can be used for development and operation of the RCP model and also it will be suitable data to evaluate the performance.

REFERENCES

[1] J. Y. Gu, K. Y. Suh, "Performance Analysis of Primary System Coolant Pump for Advanced Power Reactor," *Proc. NTHAS 2008*, Okinawa, Japan, 2008

[2] E. S. Yoon, *et al*, "Performance Evaluation of a Main Coolant Pump for the Modular Nuclear Reactor by Computational Fluid Dynamics," *J. Mechanical Science and Technology*, Part B Vol. 30, No. 8, pp. 818, 2003.

[3] ANSYS CFX Release 11.0 User Manual, 2006.